An Experimental and Numerical Investigation of the Duct Flow with an Inclined Jet Injection

Ryota YANO, Kogakuin University, Nakano-machi 2665, Hachioji, 192 Tokyo, Japan
Akisato MIZUNO, Kogakuin University
Jun-ichi SATO, Kogakuin University

Experimental and numerical study is carried out to clarify the duct flow with an inclined jet injection, as the model test of tunnel ventilation facility. A 8,800mm long duct with 230mm x 230mm square cross section is constructed, and an injection nozzle with 20mm x 230mm outlet with the angle of 30° is installed at 2,100mm from the inlet. In addition to full span injection, the nozzle with 80% span is installed to observe the effect of three dimensionality. Measured pressure gains under various flow ratios showed good agreement with the theory based on the law of momentum. The velocity distribution with full span injection showed the existence of two dimensional separation bubble, while partial injection cases revealed a stronger down wash. Numerical simulation was carried out and it was confirmed that a good qualitative agreement existed.

1. INTRODUCTION

Inclined jet injection is applied to longitudinal tunnel ventilation, in order to induce flow in the tunnel. Generally, the pressure rise effect of the ventilators, such as jet fans and large scale fans at the vertical shaft, is estimated by theoretical formulae induced by momentum theory[(1)(2)(3)(4)]. However, the pressure characteristics of the duct flow with an inclined jet, as well as the velocity field, is not yet known well, and a systematic study is considered to be necessary.

In the present paper the authors carry out a series of model experiment with a scale of 1/30, and the pressure gain performance is measured and compared with theory. The flowfield and the mixing process after the injection is also measured in detail to find out to which extent the high velocity air flow can affect the traffic in the actual tunnel. In the current experiment, the Reynolds number is smaller in comparison to the one in the actual phenomena, the authors consider that the intrinsic characteristics are common with the actual system.

Numerical simulation is carried out under the same conditions as in the experimental ones, in order to confirm the accuracy of a commercial code for the analysis of turbulent flow field.

2. NOMENCLATURE

A：Cross sectional area of the duct
A_j：Area of jet exhaust
C_p：Pressure coefficient
D：Hydraulic diameter
P：Pressure
Q_1：Flow rate in the upper stream
Q_2：Flow rate in the down stream
Q_j：Injection flow rate
Re：Reynolds number $=V_2D / \nu$
V：Velocity measured by a Pitot tube
V_1：Mean velocity in the upper stream
V_2：Mean velocity in the down stream
V_j：Jet velocity
ΔC_p：Coefficient of pressure gain
κ：Flow ratio $=Q_j / Q_2$
ρ：Air density
ψ：Area ratio $=A_j / A$

3. METHOD AND CONDITIONS OF ANALYSIS

3.1 Experimental apparatus

Fig. 1 shows the coordinate system of the apparatus, in which the main flow direction is z. A side view of the whole apparatus is illustrated in Fig. 2. The main duct has a cross section of 230mm x 230mm square (For a square, the side length is equal to hydraulic diameter, which is taken as the reference length). with a bell-mouth and honeycomb/mesh combination at the inlet. Total length of the experimental setup is 8,800mm with 7,700mm straight duct, made of plexi-glass. The exhaust fan at the end of the duct is driven by an inverter to control the main flow to be in the range from 4.0 to 13 m/s. The Reynolds numbers correspond from 6.6×10^4 to 2.1×10^5 respectively. An inclined air jet is blown into the main duct at 2,100mm downstream from the inlet, with the angel of 30°, which is the case often used in practical tunnels. The flow velocity of the jet can be set arbitrarily. The flow rate of the main duct is set to the prescribed value in terms of pressure difference of the inlet bellmouth, based on the calibration by measuring the flow rate as the integration of the velocity distribution.

The ratio of flow rates of jet injection to the main flow downstream is defined as κ, taking the range of 0 to 0.5, adding an extreme case of $\kappa=1.0$, where inlet flow to the main duct is closed. The authors prepared two nozzles in order to compare two- and three-dimensional injections. Both has a gap of 20mm and a width of 230mm for full span injection, which produces nearly two-dimensional flow, and of 184mm for partial injection (spanwise contraction to 80% of the original injection area), in which a strong

three-dimensionality is expected.

3.2 Method and conditions of numerical analysis

Numerical analysis is carried out under the same scale and parameters as in the experiment. In all cases full three dimensional analysis is performed in the half symmetrical region. However, the length of the downstream duct is set to be 10 m in the numerical simulation, because a linear pressure distribution is attained the further downstream, on which detailed discussion appears in the later section.

A commercial code is used based on finite volume method with SIMPLE algorithm[5] and k- ε model[6][7][8] for turbulence model.

4. THEORETICAL CONSIDERATION

The inflow and outflow momentum through the control surface shown in Fig. 3 are

$$M_{in} = \rho Q_1 V_1 + \rho Q_j V_j \cos\beta , \qquad (1)$$

$$M_{out} = \rho Q_2 V_2 , \qquad (2)$$

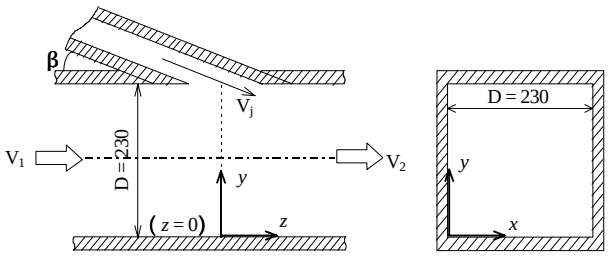

Fig. 1 Coordinate system

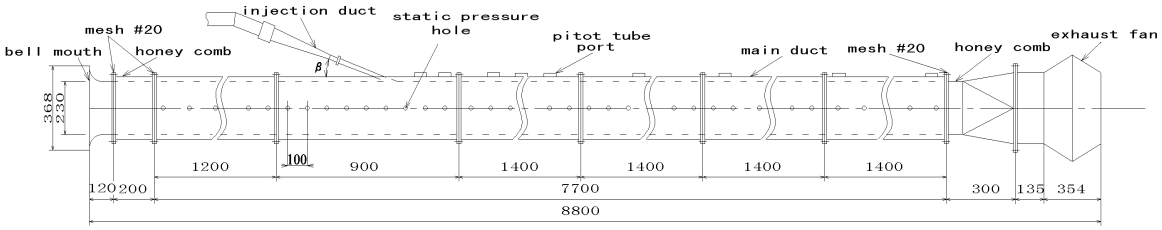

Fig. 2 Experimental apparatus

in which downstream surface is taken to be far from the injection. Hence, the pressure difference is given by momentum theory in the form

$$A\left(P_2 - P_1\right) = \rho Q_1 V_1 + \rho Q_j V_j \cos\beta - \rho Q_2 V_2 , \quad (3)$$

where

$$V_1 = \left(Q_2 - Q_j\right)\big/ A\,, \qquad (4)$$

$$V_2 = Q_2 \big/ A\,. \qquad (5)$$

By substituting Eqs. (4) and (5) into Eqs. (3), the pressure gain

$$\Delta P = 2\frac{Q_j}{Q_2}\left\{\frac{Q_j}{Q_2} + \frac{V_j \cos\beta}{V_2} - 2\right\}\frac{1}{2}\rho {V_2}^2 \qquad (6)$$

is obtained. It is converted in terms of flow ratio κ and area ratio ψ to the expression,

$$\Delta P = 2\kappa\left\{\kappa + \frac{\kappa}{\varphi}\cos\beta - 2\right\}\frac{1}{2}\rho {V_2}^2\,. \qquad (7)$$

The non-dimensional pressure gain is therefore obtained by dividing Eq. (7) with the dynamic pressure based on the downstream mean velocity $\left(\rho {V_2}^2/2\right)$ as

$$\Delta C_p = 2\kappa\left\{\kappa + \frac{\kappa}{\varphi}\cos\beta - 2\right\}. \qquad (8)$$

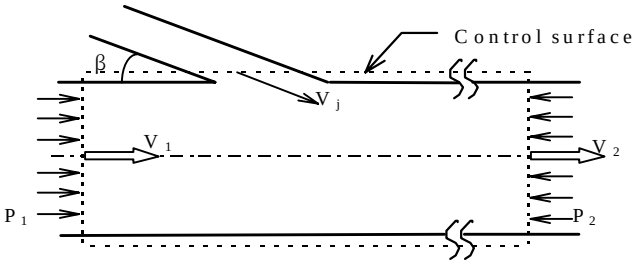

Fig. 3 Application of momentum law

5. PRESSURE DISTRIBUTION

5.1 Measured pressure distribution

The pressure distribution along the *z*-axis is measured through the pressure holes every 100mm at the height of 115mm. The diameter of the pressure hole is 1mm. The *z*-axis is

normalized by the reference length D, while the pressures are normalized by the dynamic pressure of the mean downstream velocity, $\left(\rho V_2^2/2\right)$, giving the pressure coefficient C_p. A sample distribution is shown in Fig. 4 for the κ=0.310 case. The pressure decreases linearly from the beginning to the injection nozzle. After the injection (z=0D), the pressure rises to be the highest value some 15D downstream, from which it again decreases linearly with a slightly larger inclination. In Fig. 4, the process of obtaining pressure gain is explained. Fitted lines at both sides of the injection are extrapolated to the coordinate z=0, and the pressure gain is given as the difference at the location as ΔC_p. In this process least square method is used and the data in the range from -6D to -0.4D and from 14D to 23D are used, where the data are well on straight lines with different inclinations for all the cases. The experimental pressure gains are compared with the theoretical ones in the later section.

Figures 5 is the results under partial injection, which does not show much difference with the former results.

5.2 Pressure distribution by numerical simulation

The pressure distribution obtained by the numerical analysis is illustrated in Fig. 6 and 7, in which pressure is normalized as was done in the process of experimental data. It is seen that the pressure gain by the injection and pipe friction loss can be observed in both full span injection and partial injection cases.

In the calculated pressure distribution, 15D to 25D was necessary until a linear distribution is recovered, which is much larger in comparison to experimental cases. This is the reason why we had to take 10 m (43.4D) downstream of the injection as the calculation region.

By comparing Fig.4 and Fig.6 one can observe that the experimental distribution shows a drop at the injection before rising afterwards, while it jumps up in the numerical result. In the partial injection, similar distributions between experiment and calculation are seen in the injection region.

6. COMPARISON OF THE PRESSURE GAINS

Non-dimensional pressure gain vs. flow ratio is depicted in Figs. 8 and 9. Experimental results are plotted on the theoretical curve, and they agree well in both cases. The friction loss, observed in Refs. (3) and (4), is not marked in the current results, presumably because the inclined jet loses less momentum due to wall friction.

In the same figures, numerical results are plotted with white triangles. They also show good agreement with theory, but they generally take lower values.

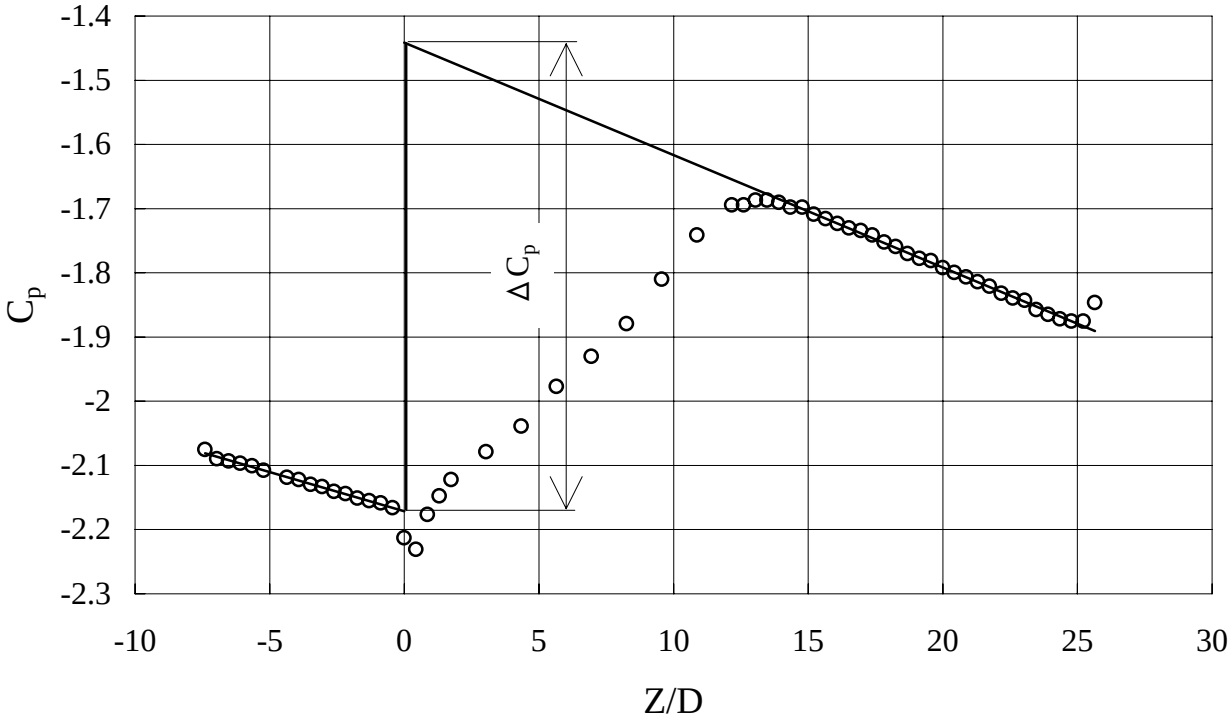

Fig. 4 Distribution of pressure coefficient
(experiment , full span injection κ =0.310)
(Explanation how to obtain pressure gain)

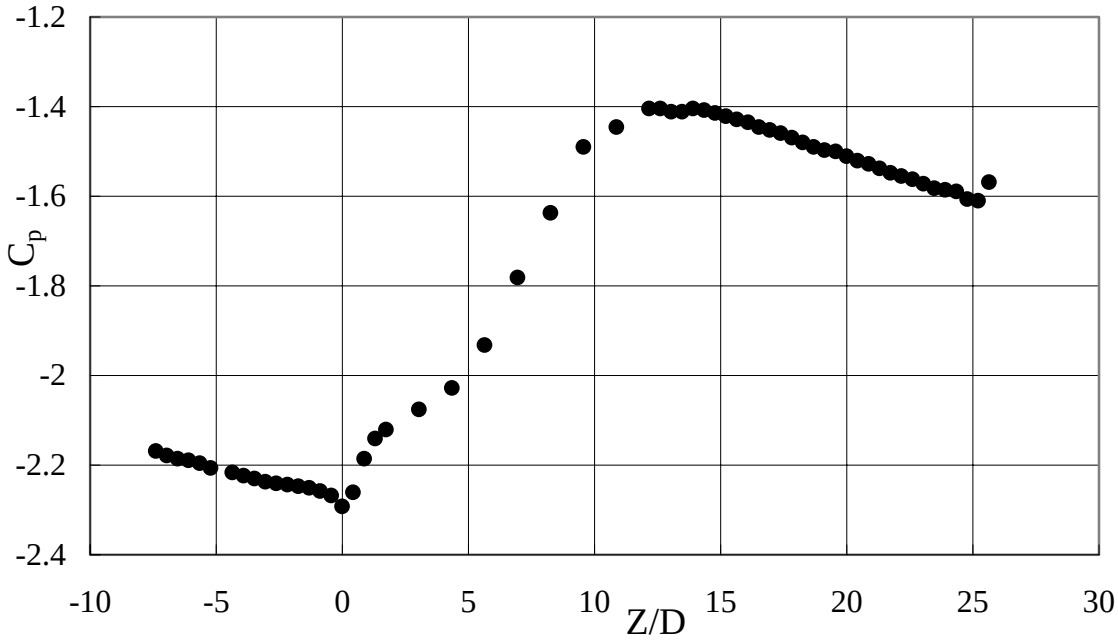

Fig. 5 Distribution of pressure coefficient

(experiment , partial span injection κ =0.280)

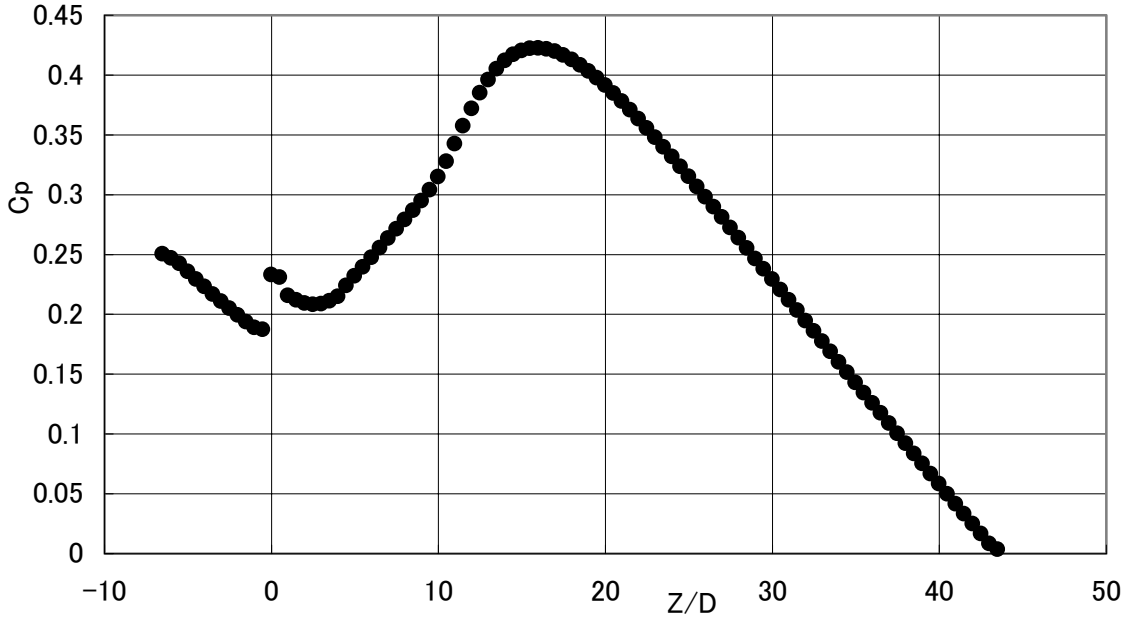

Fig. 6 Distribution of pressure coefficient
(calculation , full span injection κ =0.310)

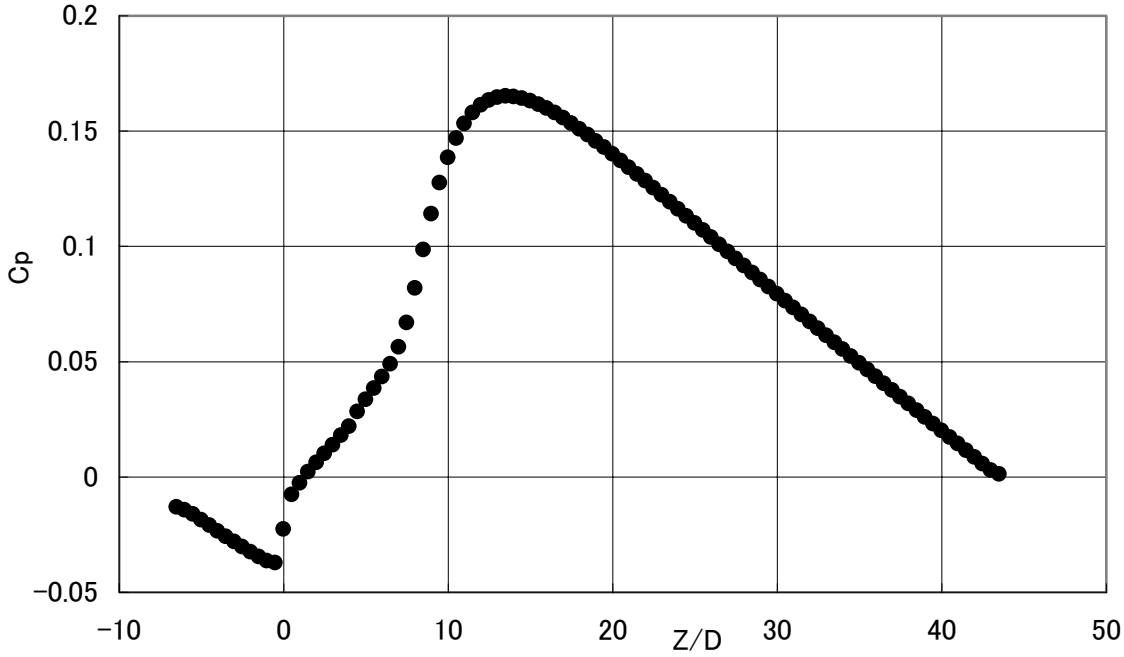

Fig. 7 Distribution of pressure coefficient
(calculation , partial span injection κ =0.280)

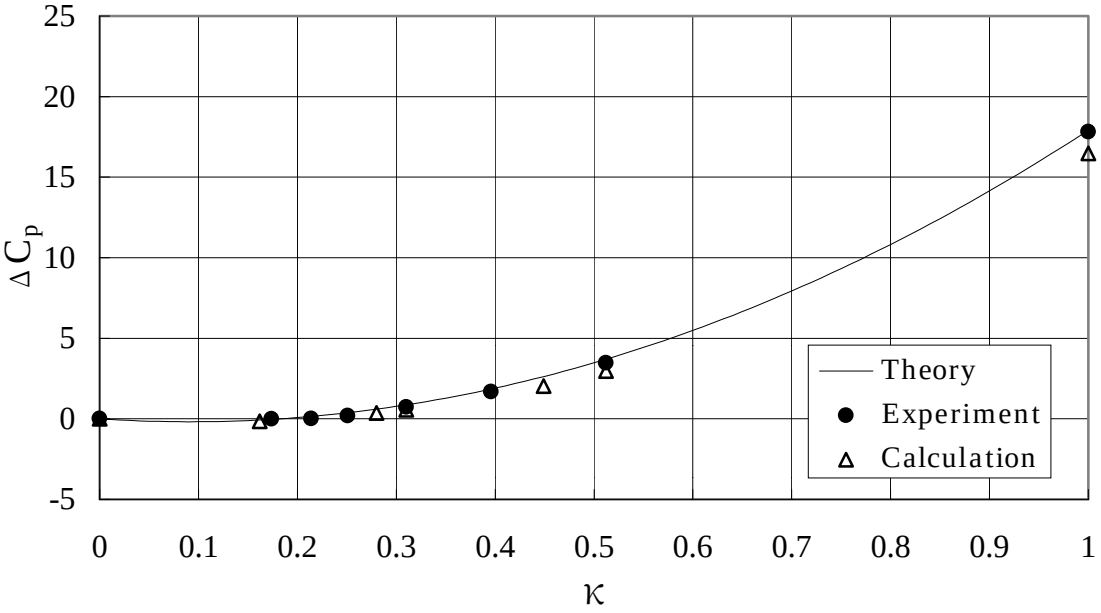

Fig. 8 Coefficient of pressure gain
(full span injection)

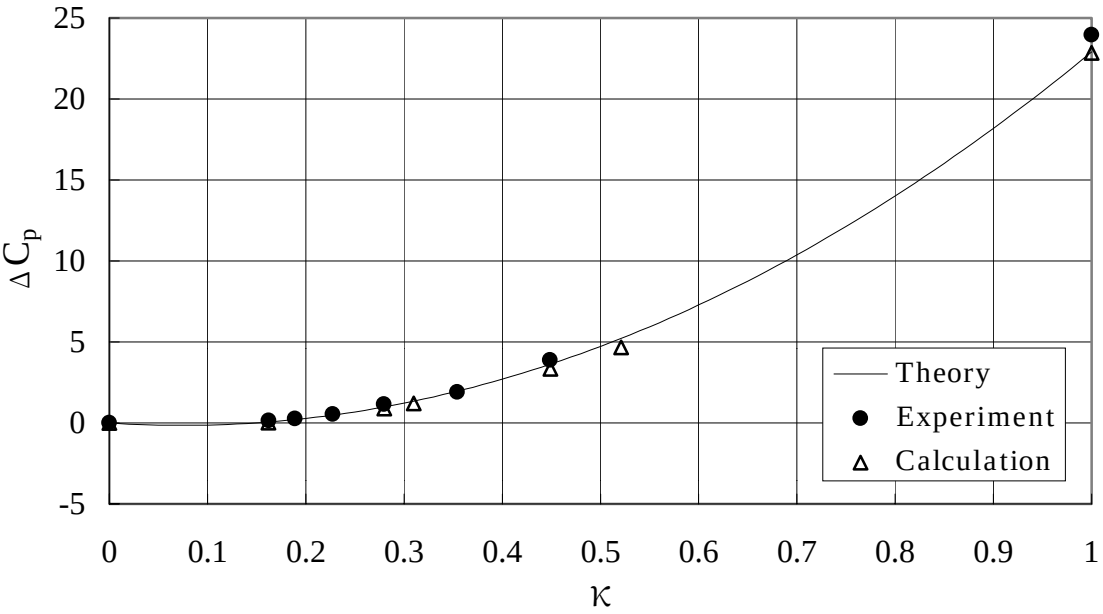

Fig.9 Coefficient of pressure gain
(partial span injection)

7. VELOCITY DISTRIBUTION

7.1 Velocity distribution by experiment

Measurement of velocity distribution is carried out at the sections of 0.5*D*, 1*D*, 2*D*, 3*D*, 5*D*, 10*D*, 15*D* and 20*D*. In the Fig. 10 the velocity distribution is shown in the case of ψ = 0.087 (full span injection), in which velocity is normalized with the downstream mean velocity V_2. The mixing process of the injected flow is observed in the figures. The injected flow has a high velocity and confined in the upper wall region, then loses the speed gradually by turbulent mixing, while it flows downstream.

The velocity profiles for partial injection are shown in Fig. 11, in which the area ratio ψ is 0.070. By comparing the case of κ=0.280 (Fig. 11) with the counterpart with similar flow ratio (Fig. 10), it is noted that higher velocity region reaches closer to the bottom wall at cross section of *z*=2*D* to 5*D*, due to three-dimensionality. As the injection area is 80% of the span, it is less likely that a closed separation bubble is composed, which caused this tendency.

7.2 Velocity distribution by numerical simulation

The velocity distributions by numerical simulation are shown in Figs. 12 and 13. In the partial span injection case, higher velocity reached downward in comparison to full span injection case, as was observed in the experiment. The effect of the jet diminishes at around 20*D* in the experimental results, while it does not in the numerical one, both in full span and partial span injection cases.

8. CONCLUSION

Experimental investigation was carried out of the pressure gain measurement of an inclined jet injection into a square duct under various flow ratios and nozzle widths. The pressure gains showed good agreement with the theoretical values. This is due to a smaller wall friction in comparison to the former works, where the injection was parallel to the wall.

By injecting from the nozzle with 80% span of the duct, the velocity distribution spread to the area further from the ceiling than the one with full span injection. This is obviously due to being three dimensional flow, and a high velocity region spreads downward. As the experiment was carried out at a lower Reynolds number than the actual case, which may lead to minor discrepancy, one may be requested to be cautious for the application to the actual system.

Numerical simulation was carried out, and pressure distribution and velocity distribution are analyzed. They gave good agreement with experiment or theory quantitatively, but further study for the improvement of the applicability of the numerical code seemed to be necessary.

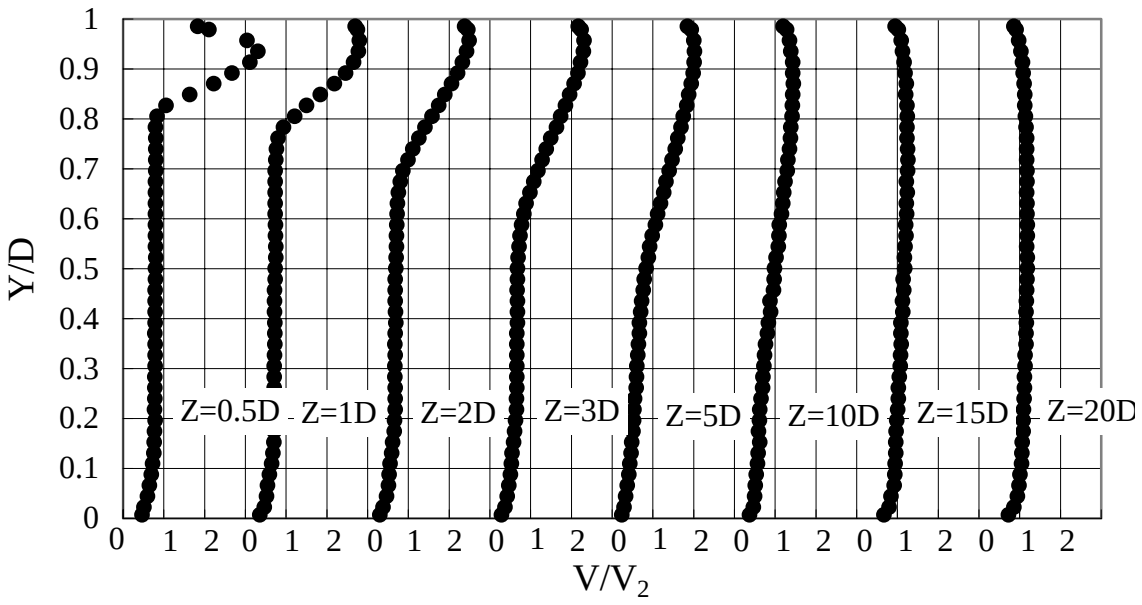

Fig. 10 Velocity distribution
(experiment , full span injection κ =0.310)

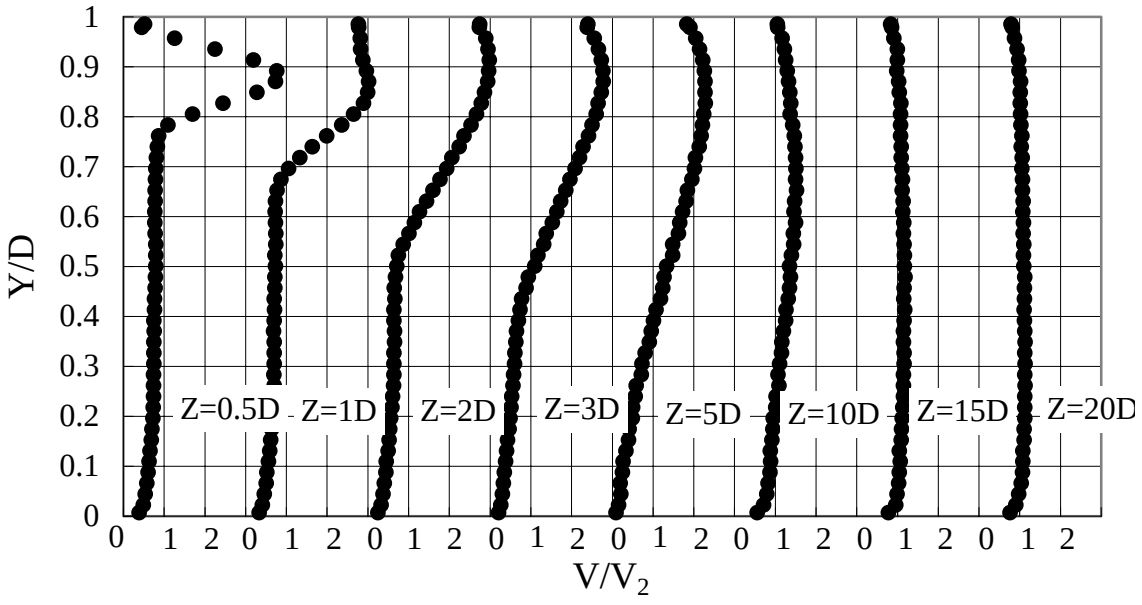

Fig. 11 Velocity distribution
(experiment , partial span injection κ =0.280)

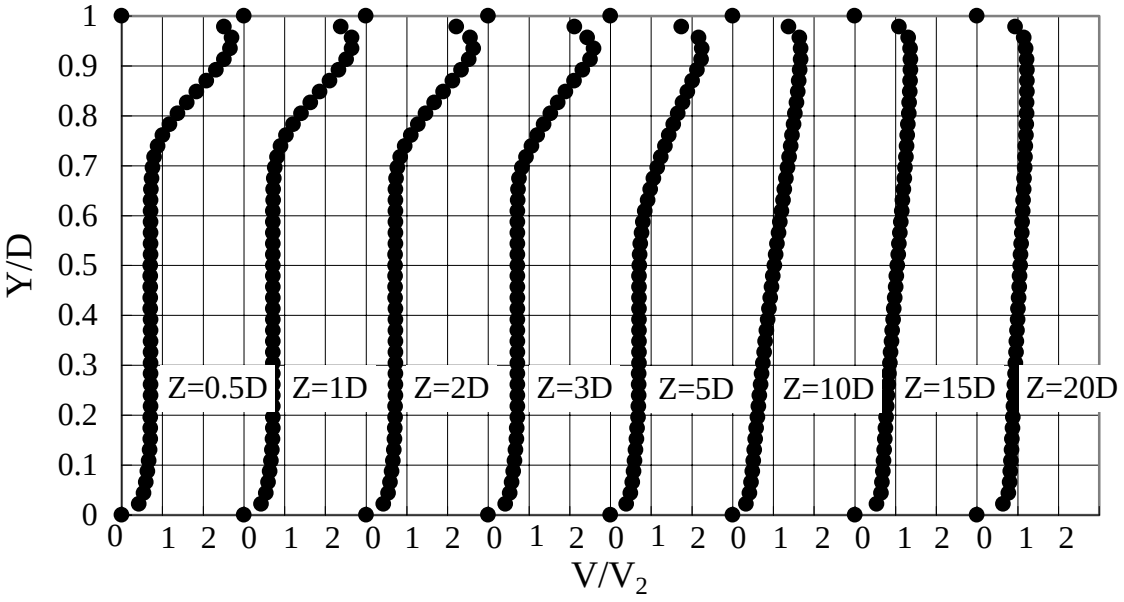

Fig. 12 Velocity distribution
(calculation , full span injection κ =0.310)

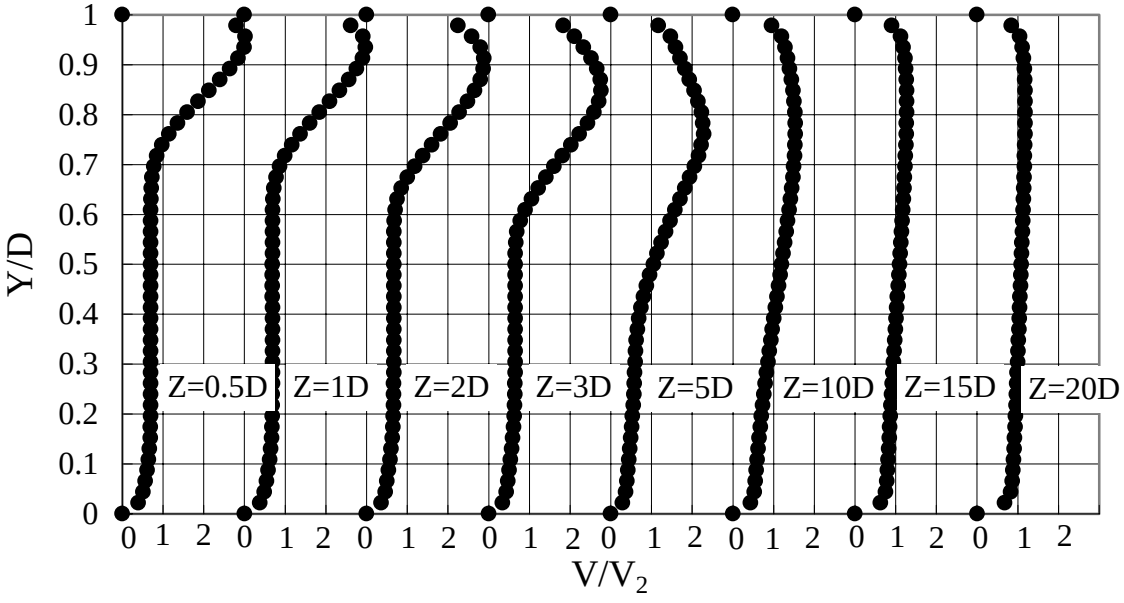

Fig. 13 Velocity distribution
(calculation , partial span injection κ =0.280)

REFERENCES

(1) Japan Road Association(ed.)., Techinical guideline of road tunnels (ventilation), (in Japanese), Maruzen Co., (1985).

(2) Technology Center of Metropolitan Expressway., Report on Survey and Research on Tunnel Ventilation Design Principles, Metropolitan Expressway Public Corporation (1993).

(3) Mizuno, A. and Araie, K., Measurement of Pressure Rise Performance of a Jet Fan in a Tunnel by Model Experiment, Trans. Jpn. Soc. Mech. Eng., (in Japanese), Vol. 55, No. 514, B (1988), pp. 1613-1617.

(4) Mizuno, A. Araie, K. and Osato, H., Pressure Rise Effect by an Electrostatic Precipitator Station at Tunnel Crown, Trans. Jpn. Soc. Mech. Eng., (in Japanese), Vol. 56, No. 530, B (1989), pp. 3012-3017.

(5) Rodi, W., Influence of buoyancy and rotation on equations for turbulent length scale, Proc. 2nd Symp. on Turbulent Shear Flows, (1979).

(6) El Tahry, S.H., K- ε equation for compressible reciprocating engine flows, AIAA J.Energy, 7, No.4,(1983), pp.345-353.

(7) Patankar, S.V., and Spalding, D.B., A calculation procedure for heat, mass and momentum in three-dimensional parabolic flows, Int. J. Heat Mass Transfer, 15, (1972).

(8) Launder, B. E., and Spalding, D. B. The numerical computation of turbulent flow, Comp. Meth. in Appl. Mech. &Eng., 3, p.269, (1974).